

Electronic Structure of Te/Sb/Ge and Sb/Te/Ge Multi Layer Films Using Photoelectron Spectroscopy

Ju Heyuck Baek,[†] Young-kun Ann,[†] Kwang-Ho Jeong,[†] Mann-Ho Cho,^{*,†}
Dae-Hong Ko,[‡] Jae-Hee Oh,[§] and Hongsik Jeong[§]

Institute of Physics and Applied Physics, Yonsei University, Seoul 120-749, Korea, Department of Material Science and Engineering, Yonsei University, Seoul 120-749, Korea, and Technology Development Team, Samsung Semiconductor Memory Institute, Kiheng 449-711, Korea

Received March 2, 2009; E-mail: mh.cho@yonsei.ac.kr

Abstract: Te/Sb/Ge and Sb/Te/Ge multilayer films with an atomically controlled interface were synthesized using effusion cell and e-beam techniques. The layers interacted during the deposition, resulting in films composed of Sb–Te–Sb–Sb/Ge and Sb/Sb–Te/Ge–Te/Ge respectively. Atomic diffusion and chemical reactions in films during the annealing process were investigated by photoemission spectroscopy. In the case of Te/Sb/Ge, Ge diffused into the Sb–Te region released Sb in Sb–Te bonds and interacted with residual Te, resulting in a change in valence band line shape, which was similar to that of a Ge₁Sb₂Te₄ crystalline phase. The Ge–Sb–Te alloy underwent a stoichiometric change during the process, resulting in a 1.2:2:4 ratio, consistent with the most stable stoichiometry value calculated by ab initio density-functional theory. The experimental results strongly suggest that the most stable structure is generated through a reaction process involving the minimization of total energy. In addition, Ge in the Sb/Te/Ge film diffused into Sb–Te region by thermal energy. However, Ge was not able to diffuse to the near surface because Sb atoms of the high concentration at the surface were easily segregated and hindered the diffusion of other elements.

Introduction

Te-based phase-change alloys have been extensively studied for use in next generation memory devices for mobile and digital equipment because of their nonvolatility and high performance characteristics. The most commonly used phase change materials are Ge–Sb–Te ternary alloys which show pronounced differences in electrical conductivity and optical reflectivity between the amorphous and crystalline states.^{1,2} Moreover, the speed of the phase transformation is very fast within the nanosecond time scale, indicating that it is potentially applicable for use in memory devices, that is, phase change random access memory (PC-RAM) using Ge–Sb–Te alloy is considered to be essentially close to practical use.^{3–5} The crystalline structure of Ge–Te–Sb alloys is thought to be a metastable crystalline state, which is a distorted rocksalt structure with the B site being fully occupied by Te and the A site being randomly occupied by Sb, Ge and vacancies. The occupation of vacancies has continuous values ranging from 0 to 20% depending on the ratio of GeTe

and Sb₂Te₃ in the crystal structure.⁶ It is currently thought that the vacancy concentration is related to the phase transition speed and energy from the amorphous to the crystalline state as evidenced by computational approaches. In order to improve the energetic stability and transition speed of Ge–Sb–Te compounds, except for the well-known pseudobinary alloys such as GeTe, Ge₁Sb₂Te₄, Ge₁Sb₄Te₇, and Ge₂Sb₂Te₅, numerous compounds with various compositions have been actively studied through modification of the continual vacancy number.^{7–10} However, the majority of such studies have been mainly involved theoretical calculations using density functional theory related to the role of vacancies determined by stoichiometry of the Ge–Sb–Te film.¹¹ Unfortunately, systematic experimental data to support the theoretical calculations related to the electronic structure have not yet been reported. In this paper, we report on an investigation of changes in the chemical bonding state and electronic structure of some Ge–Sb–Te alloys that occur as the result of interfacial reactions and interdiffusion. The experimental findings are based on the preparation of atomically controlled layered structures and photoemission

[†] Institute of Physics and Applied Physics, Yonsei University.

[‡] Department of Material Science and Engineering, Yonsei University.

[§] Samsung Semiconductor Memory Institute.

(1) Ovshinsky, S. R. *Phys. Rev. Lett.* **1968**, *21*, 1450–1453.

(2) Wuttig, M. *Nat. Mater.* **2005**, *4*, 265–266.

(3) Yamada, N.; Ohno, E.; Nishiuchi, K.; Akahira, N.; Takao, M. *J. Appl. Phys.* **1991**, *69*, 2849–2856.

(4) Pirovano, A.; Lacaíta, A. L.; Benvenuti, A.; Pellizzer, F.; Bez, R. *IEEE Trans. Electron Devices* **2004**, *51*, 452–459.

(5) Redaelli, A.; Pirovano, A.; Pellizzer, E.; Lacaíta, A. L.; Ielmini, D.; Bez, R. *IEEE Electron Device Lett.* **2004**, *25*, 684–686.

(6) Matsunaga, T.; Yamada, N. *Jpn. J. Appl. Phys.* **1 2002**, *41*, 1674–1678.

(7) Matsunaga, T.; Kojima, R.; Yamada, N.; Kifune, K.; Kubota, Y.; Tabata, Y.; Takata, M. *Inorg. Chem.* **2006**, *45*, 2235–2241.

(8) Jung, Y.; Lee, S. H.; Ko, D. K.; Agarwal, R. *J. Am. Chem. Soc.* **2006**, *128*, 14026–14027.

(9) Lee, J. S.; Britzman, S.; Yu, D.; Park, H. *J. Am. Chem. Soc.* **2008**, *130*, 6252–6258.

(10) Yu, D.; Wu, J. Q.; Gu, Q.; Park, H. K. *J. Am. Chem. Soc.* **2006**, *128*, 8148–8149.

(11) Wuttig, M.; Lusebrink, D.; Wamwangi, D.; Welnic, W.; Gillissen, M.; Dronskowski, R. *Nat. Mater.* **2007**, *6*, 122–128.

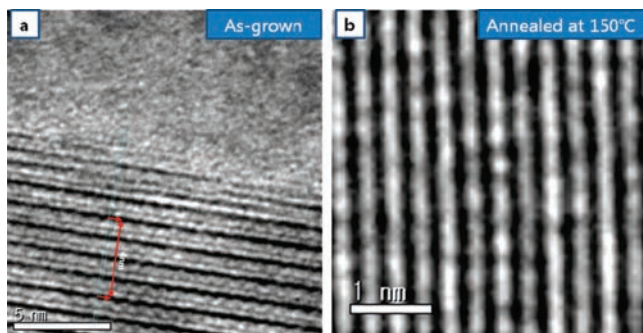


Figure 1. Cross-sectional TEM images of (a) as-deposited and (b) 150 °C annealed multilayer films with a unit structure of Te(9 Å)/Ge(8 Å)/Te(9 Å)/Sb(8 Å).

experiments. The findings provide information concerning the role of the each element for achieving the most stable stoichiometry through systematic changes in electronic structure at various temperatures.

Experimental Section

Confirmation of Atomically Controlled Multilayer. To design a useful phase change material and to investigate reactions among the elements, the film thickness of amorphous multilayer films with a unit structure of Te(9 Å)/Ge(8 Å)/Te(9 Å)/Sb(8 Å) was determined by considering the atomic weight and density for the formation of stoichiometric $\text{Ge}_2\text{Sb}_2\text{Te}_5$. The thickness of the multilayer films were controlled by automatic shelters connected to a quiz thickness controller. We also confirmed the uniformity of the atomic controlled film from cross-sectional TEM (transmittance electron microscopy) images, as shown in the Figure 1a. In the as-grown stacked layers, the thickness of the unit structure is about 4 nm and the interfaces of the multilayer can be clearly observed. X-ray diffraction (XRD) patterns of the specimen were also consistent with the presence of an amorphous state (see Figure S1 in Supporting Information). After an annealing treatment at a temperature of 150 °C, we found that it was possible to control the phase transition from the amorphous to the crystal phase through atomic diffusion between the heterolayers, as shown in Figure 1b. XRD measurements (see Figure S1 in Supporting Information) indicated that the metastable fcc structure¹² of Ge–Sb–Te alloy was crystallized, well ordered state. The results show that it is possible to grow uniformed multilayer that can be used in photoemission experiments.

Preparation of Multilayer Films for Photoemission Experiment. To investigate changes in the electronic structure through the diffusion process, we fabricated various multilayer films, such as Te/Ge, Sb/Te/Ge, Sb/Te, Sb/Ge, Te/Sb/Ge and Te/Sb structures. A 30 nm thick Ge film and a 15 nm thick Sb(Te) film were deposited on a Si(001) substrate using e-beam growth and thermal effusion cell method, respectively. The base pressures of the growth chambers were maintained below 1×10^{-9} torr. The Te(Sb) layer (1, 3, 5, 7 and 10 Å) was subsequently grown on Sb(Te) film of the thick 15 nm or cleaned Ge film and in the case of multilayer comprised of three elements, Sb(Te) layer (1, 3, 5, 7 and 10 Å) was grown on Te(Sb)/Ge in a stepwise manner. The growth chamber was connected to an analysis chamber for photoemission experiments to permit XPS (X-ray photoemission spectroscopy) and UPS (Ultraviolet photoemission spectroscopy) spectra of the film to be collected without interrupting the vacuum. The thickness of each layer deposited was monitored using a calibrated quartz thickness monitor.

Photoemission Experiment. The chemical bonding state and electron structure of the films at each thickness were investigated

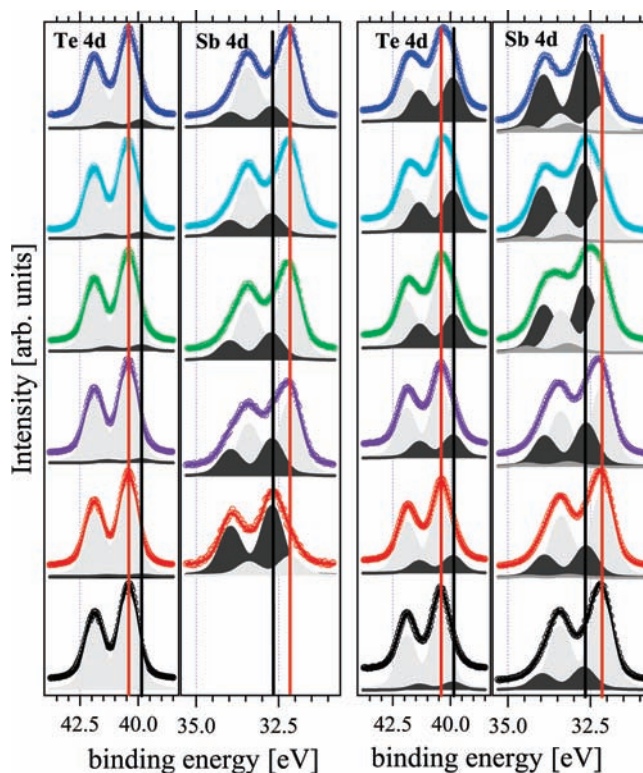


Figure 2. (a) Core-level spectra of Te 4d and Sb 4d obtained with 1, 3, 5, 7 and 10 Å-thick Sb deposited on the Te(150 Å)/Si and (b) Sb(10 Å)/Te(150 Å)/Si annealed at as-deposition, 100 °C, 120 °C, 150 °C, 200 °C and returned to room-temperature.

by monochromatic X-ray (Al $K\alpha$) and an unfiltered UV (He I) source. After the deposition, to observe atomic diffusion and chemical reactions of each element, the multilayer films in a spectral chamber were investigated using XPS and UPS at isothermal temperatures of 100, 120, 150, and 200 °C and were then returned to room-temperature. The Fermi edge was determined from UPS and XPS spectra collected on the clean Au sample in electrical contact with the Ge, Sb and Te sample and the core level energy was calibrated by clean Au 4f (83.9 eV).

Analytic Method. On the basis of changes in XPS spectra with each thickness and annealing temperature, gradual changes in the chemical reaction were clearly observed in the core level spectrum with Sb 4d and Te 4d, as shown in Figure 2. In the samples deposited with Sb thicknesses of 1, 3, 5, 7 and 10 Å on a 150 Å thick Te layer, the spectrum of Sb 4d was easily deconvoluted by the metallic bonding (32.15 eV) and Sb–Te bonding (32.75 eV) state.^{13,14} The analyzed spectrum showed that the peak height of the Sb–Te bond was saturated before approaching the Sb film thickness to 3 Å and the peak of Sb–Sb bond was continuously increased over the film thickness of \sim Sb 3 Å (the ratio of Sb–Sb to Sb–Te was 0.25, 2.2, 3.35, 4.1, and 4.2 at each thickness). In the Te 4d spectrum, no significant change in the Te–Sb bonding component was observed, because the peak height of Te–Sb bonds was lower than that of the Te–Te metallic bonds in a 150 Å thick Te layer. The deconvolution process indicated that the layer structure of the multi layer was composed of Sb–Sb($>$ 7 Å)/Sb–Te($<$ 3 Å)/Te. After the annealing process, the continuous change in the peaks indicates that chemical reactions had occurred through atomic diffusion, as shown in Figure 2 at the right side. We calculated the changes in stoichiometry and the electronic

(12) Ie, S. Y.; Bea, B. T.; Ahn, Y. K.; Chang, M. Y.; You, D. G.; Cho, M. H.; Jeong, K. *Appl. Phys. Lett.* **2007**, *90*, 251917.

(13) Pollak, R. A.; Kowalczyk, S.; Ley, L.; Shirley, D. A. *Phys. Rev. Lett.* **1972**, *29*, 274–277.

(14) Shalvoy, R. B.; Fisher, G. B.; Stiles, P. J. *Phys. Rev. B* **1977**, *15*, 1680–1697.

structure in the film using the deconvoluted Sb 4d and Te 4d spectrum before and after diffusion. In the Sb 4d and Te 4d spectrum, a portion of the Sb–Te bonding state increased by 200 °C and the stoichiometry of Sb:Te changed from 2.1:1 to 2:2.6. From these results, we concluded that a stable $\text{Sb}_2\text{Te}_{2.6}$ alloy was generated by inter diffusion at an annealing temperature of 200 °C. On the basis of this method of analysis, it was possible to analyze the electronic structure of each film formed from the Ge, Sb, and Te layered structure.

Results and Discussion

To examine the quantitative changes in electronic structure and stoichiometry before and after the annealing process, we confirmed the existence of a layer structure of all synthesized multi layer films. For references to the homopolar bonding states, Ge 3d, Sb 4d and Te 4d spectrum were obtained in single-layer films composed of each element of Ge, Sb and Te, as shown in Figure 3a. On the basis of the results, the relative binding energy scale is referenced to each $3d_{5/2}$ and $4d_{5/2}$ core level of the major metallic binding energy ($\text{Ge}3d_{5/2} = 29.4$ eV, $\text{Sb}4d_{5/2} = 32.15$ eV and $\text{Te}4d_{5/2} = 40.4$ eV).^{13,14} In the case of a multi layer film of Sb(10 Å)/Ge, as shown in Figure 3e, no shift in the core level energy state could be found, except for the reduced intensity of the Ge 3d peak caused by Sb coverage, resulting in the absence of any chemical reaction of the Ge–Sb between Ge and Sb layer. On the other hand, depositing Te on the Sb(10 Å)/Ge sample, as shown in Figure 3f, the spectra of Sb 4d was changed significantly, resulting in the deconvolution of Sb 4d with Sb–Te (+0.6 eV) and a metallic bonding state. In particular, the component portion of the Sb–Te bond increased continually until the thickness of the Te layer reached 10 Å. The change in the spectrum of Te 4d also reflected the change in the Sb 4d bonding state (Te–Sb: –0.55 eV). In the case of another multi layer film of Sb(10 Å)/Te(10 Å)/Ge, the Sb 4d spectrum was mainly composed of the Sb–Sb bonding component as shown in Figure 3c, while the Sb–Te bonding state component was saturated when the thickness of Sb layer reached 3 Å (see Figure S2 in Supporting Information). The difference between the two samples of Te/Sb/Ge and Sb/Te/Ge can be explained in the case of Te(10 Å)/Ge film, as shown in Figure 3b. Comparing the Te 4d spectrum of Te(10 Å)/Ge with that for a sample of Te/Sb/Ge, we were able to observe that a Ge–Te reaction had occurred. As the result of the reaction, the Te 4d spectrum could be deconvoluted with two components, that is, a Ge–Te bonding state with a lower binding energy (0.3 eV) and a metallic bonding state of zero position. In addition, the Ge–Te bonding state in the Ge 3d spectrum, which was shifted to 0.55 eV positive direction, was separated from the bulk homopolar bonding state. The Ge–Te reaction, however, becomes saturated when the thickness of the Te layer reaches 5 Å (see Figure S3 in Supporting Information) and the near surface is composed of Te–Te metallic bonds. Therefore, when Sb is deposited on Te/Ge, a relatively small quantity of Te contributes to the formation of Sb–Te bond, in comparison to Te deposited on Sb/Ge. Another reason for the difference could be caused by the change in the surface morphology, that is, the surface of Te layer is smoother than that of the Sb layer. As evidenced from a comparison of Figure 3d and g, in spite of the absence of a Ge layer, the Te 4d spectrum of Te(10 Å)/Sb(150 Å), and the Sb 4d spectrum of Sb(10 Å)/Te(150 Å) show that the Sb–Te reaction region of Te(10 Å)/Sb(150 Å) was thicker than that of Sb(10 Å)/Te(150 Å) (the ratio of Sb–Sb to Sb–Te component in Sb/Te film: 4.2, the ratio of the Te–Te to Te–Sb component in the Te/Sb film: 0.96). Thus, the reaction

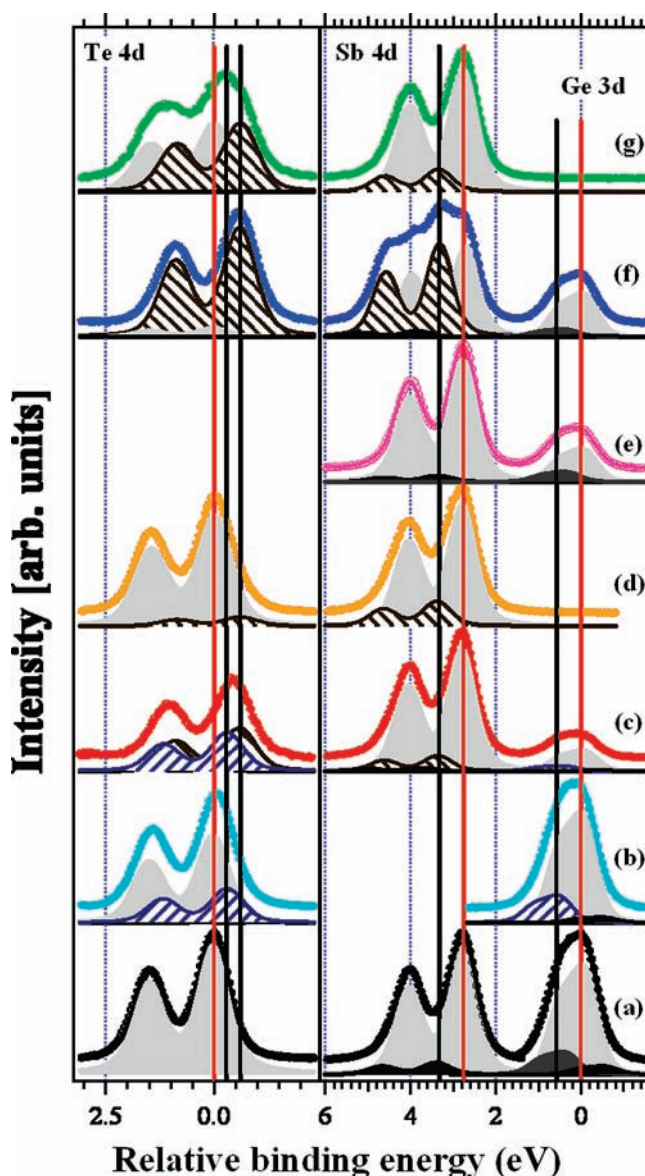


Figure 3. (a) Core -level spectra of Te 4d, Sb 4d and Ge 3d obtained for each single layered film of Te, Sb and Ge and various multilayer films such as (b) Te(10 Å)/Ge, (c) Sb(10 Å)/Te(10 Å)/Ge, (d) Sb(10 Å)/Te, (e) Sb(10 Å)/Ge, (f) Te(10 Å)/Sb(10 Å)/Ge and (g) Te(10 Å)/Sb. The circles are data points, and solid curves are fits. The relative binding energy scale is referred to the Ge 3d $3d_{5/2}$ and Te $4d_{5/2}$ binding energy of major metallic bonds.

is critically affected by the stacking sequence, that is, the interfaces of the Te(10 Å)/Sb(10 Å)/Ge and Sb(10 Å)/Te(10 Å)/Ge multi layers were actually organized by Sb–Sb + Sb–Te/Ge and Sb/Sb–Te/Ge–Te/Ge, respectively.

The interfacial reaction and structural change as a function of stack structure after the annealing treatment were also investigated. Structural changes through atomic diffusion between the confirmed interface regions had occurred during the annealing process. Changes in the chemical bonding state caused by the structural transition are closely related to the phase transition characteristics.^{11,15} Figure 4 shows the XPS chemical bonding states for the Ge 3d, Sb 4d and Te 4d core levels for multi layer films that were annealed at 200 °C. In the case of

(15) Klein, A.; Dieker, H.; Spath, B.; Fons, P.; Kolobov, A.; Steimer, C.; Wuttig, M. *Phys. Rev. Lett.* **2008**, *100*, 162402.

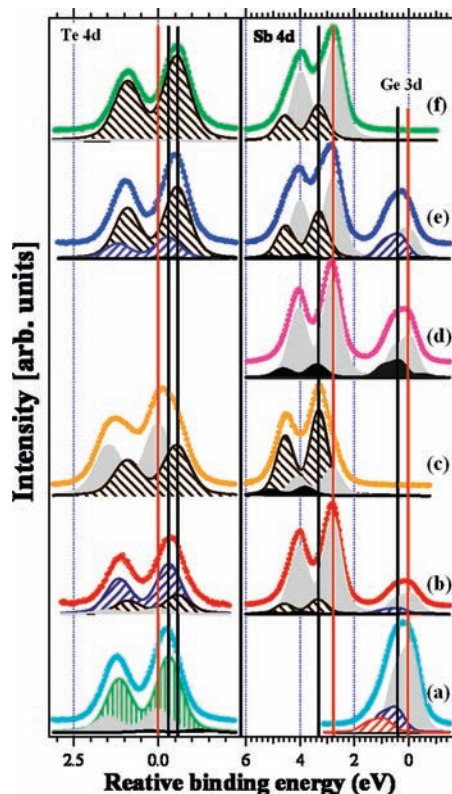


Figure 4. Te 4d, Sb 4d and Ge 3d core-level spectra of (a) Te(10 Å)/Ge, (b) Sb(10 Å)/Te(10 Å)/Ge, (c) Sb(10 Å)/Te, (d) Sb(10 Å)/Ge, (e) Te(10 Å)/Sb(10 Å)/Ge and (f) Te(10 Å)/Sb multi layer film annealed at temperature of 200 °C.

Te(10 Å)/Ge, the portion of the Ge–Te bonding state component increased, resulting from interdiffusion between the Ge and Te layers. Moreover, another component of the Ge–Te bonding state caused by the formation of *a*-GeTe₂ was observed at the +1 eV shifted position of the binding energy from the main peak of metallic bulk Ge3d, as shown in Figure 4a. Although the peaks caused by the bonding states of Ge–Te and Ge–Te₂ could not be deconvoluted in the Te 4d spectrum, the valence band spectra fully support the bonding states caused by this formation, as shown in Figure 5a. This aspect is discussed in detail below. In the Sb(10 Å)/Te(10 Å)/Ge multilayer (Figure 4b), the Ge–Te bonding component in the Te 4d spectrum clearly increases, while no significant change in the Sb4d spectrum is observed after the annealing treatment. Finally, the change in Ge 3d and Te 4d core level spectra in Sb(10 Å)/Te(10 Å)/Ge show that Ge atoms diffuse into the Sb–Te region, resulting in the formation of the Sb–Sb/Sb–Te/Ge–Te/Ge bonding states.

To investigate changes in the valence band after the annealing treatment, we used UPS by a He–I exciting light source, which shows better surface sensitivity than soft X-rays.¹⁶ The valence band spectra of a Te(10 Å)/Ge film deposited at room temperature was compared with that of an annealed film, as shown in Figure 5a. The valence band spectrum of the as-grown Te(10 Å)/Ge film shows relatively high peak height at 1.72 and 4.65 eV, shoulders at around 3.7 eV, and a clear dip at 2.77 and 6 eV with respect to the Valence-band maximum (VBM), which is very similar to that of the 5p region of a Te single layer, as shown in Figure 5 at the left side (the relatively high peak; 1.7

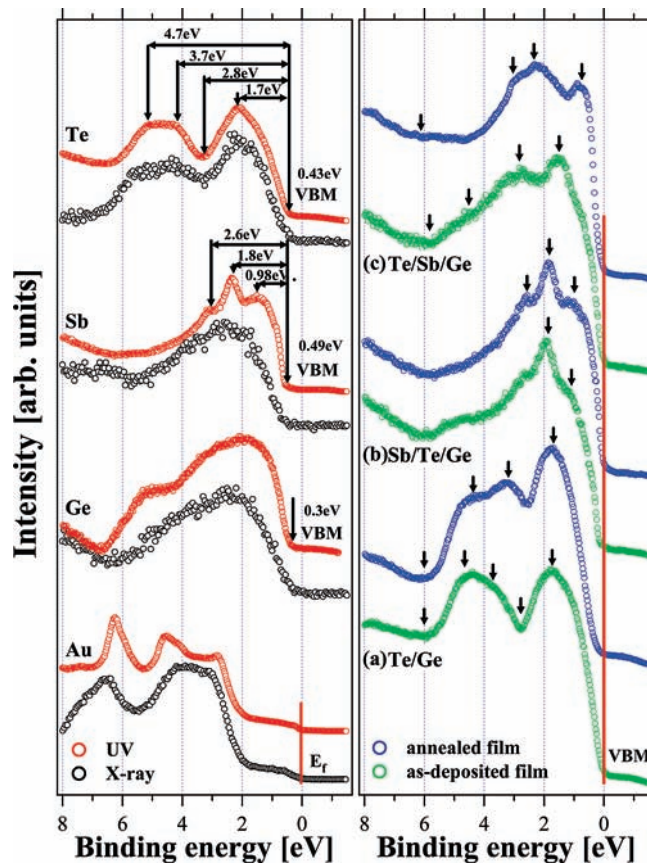


Figure 5. Valence band photoemission spectra (left) from Au, Ge, Sb and Te single layered films were recorded by X-ray (black circles) and ultraviolet (red circles) light sources. The UPS spectra (right) near the Fermi level of the as-deposited (green circles) and annealed (blue circles) films. Each spectrum was obtained from (a) Te(10 Å)/Ge, (b) Sb(10 Å)/Te(10 Å)/Ge and (c) Te(10 Å)/Sb(10 Å)/Ge films.

eV and 4.7 eV, a shoulder at around 3.7 eV, clear dip; 2.8 eV and 6 eV). Thus, the near surface of Te(10 Å)/Ge is composed of metallic Te. On the other hand, the UPS spectrum of the annealed sample shows almost same shape as that reported for amorphous GeTe, that is, the valence band of the sample is composed of peaks, 1.68 eV, 3.2 eV, and shoulders at around 4.37 eV in the Ge 4p and Te 5p region with respect to the VBM. Thus, the valence and core line shape indicates a randomly bonded 4(Ge):2(Te), which is a coordinated network model of an amorphous GeTe film.^{17,18} In the model, the Ge atoms show numerous Ge–Ge homopolar bonds and a SP³ hybridization electronic configuration with a 4-fold coordination, resulting in the formation of two bonds with only 5p electrons of Te atoms. Therefore, the electronic configuration based on valence band spectra shows that the film continuous to maintain an amorphous structure, although Ge is sufficiently diffused to the near surface of Te(10 Å)/Ge film by thermal energy. Considering the reported crystallization temperature, the phase transition occurs at 150 °C in the film with a 1:1 stoichiometry of Ge and Te, but crystallization temperature is increased to above 200 °C in the film with a Te rich stoichiometry.¹⁹ The reported results support the valence band spectrum of the amorphous state of the Ge/Te multilayer annealed at 200 °C.

(17) O'Reilly, E. P.; t, J. R.; Kelly, M. J. *Solid State Commun.* **1981**, *38*, 565–568.

(18) Hosokawa, S.; Hari, Y.; Kouchi, T.; Ono, I.; Sato, H.; Taniguchi, M.; Hiraya, A.; Takata, Y.; Kosugi, N.; Watanabe, M. *J. Phys.: Condens. Matter* **1998**, *10*, 1931–1950.

(16) Cumpson, P. J. *Surf. Interface Anal.* **1997**, *25*, 447–453.

In Figure 5b, the valence band structure of an as-grown Sb(10 Å)/Te(10 Å)/Ge film shows a shoulder at around 0.98 and 2.6 eV with respect to the VBM. After annealing the film at 200 °C, the broad shoulder at 0.98 and 2.6 eV changed to a relatively small peak. Another important finding is that the distinct fine structural peak at 1.8 eV remains unchanged even in the annealed film (a distinct peak is not found using soft X-ray beam). From the reference peak of the valence spectra in the Sb single layer, as shown in Figure 5 at the left side, the fine peak is the result of a layer comprised of only Sb–Sb bonding. Therefore, UPS spectra directly show that Sb atoms are easily segregated and other element that diffuse to the near surface are interrupted by segregated Sb in the case of high level of Sb in the Ge–Sb–Te film.^{20,21}

The another importance point can be observed in the Te(10 Å)/Sb(10 Å)/Ge multilayer, as shown in Figures 4e and 5c. Before annealing process, the chemical states of the film can be deconvoluted by the two bonding components of Sb–Te and Sb–Sb, as shown in Figure 3f. Based on the deconvoluted spectrum of Sb 4d, Te 4d and Ge 3d in Figure 4e, they show clear tendency with the annealing treatment, that is, the intensity of the Sb–Te bonding component decreases, while that of the Ge–Te component appears. The Ge–Te bonding is gradually increased with increasing annealing temperature over 150 °C (see Figure S4 in Supporting Information). On the other hand, no changes in bonding characteristics are observed for both Sb4d of Sb(10 Å)/Te and Te4d of Te(10 Å)/Sb, as shown in Figure 4c and f, respectively. Moreover, chemical reaction of Sb–Te bond in the films is enhanced continuously up to 200 °C. (see Figure S5 in Supporting Information). Therefore, the decrease in Sb–Te bonds in Te/Sb/Ge film can be explained by assuming that diffused Ge atoms expel Sb atoms in Sb–Te bonds and then interact with any residual Te atoms. In recent publication,¹¹ the total energy of a GeSbTe alloy system was calculated through the removal of either Ge or Sb from a Ge₂Sb₂Te₄ crystal, resulting in the most stable structure with the stoichiometry of a GeSbTe alloy, 1.5:2:4. The theoretical calculation shows that electrons of antibonding states of Sb–Te and Ge–Te are concentrated in the Fermi level vicinity and many electrons are concentrated into energetically unfavorable structures. In addition, the Sb–Te interactions contribute more antibonding states than the Ge–Te interactions. Thus, the reported calculation is consistent with our experimental data because our data indicate a contribution by antibonding states and an interaction mechanism through the conversion process from an energetically instable to a more stable state. The change in the bonding states of Sb–Te and Sb–Sb shows that Sb is interchanged with the diffused Ge. Moreover, this tendency increases with increasing annealing temperature up to 200 °C, indicating that the interchange process is favorable for a stable structure. Consequently, the total energy of the multilayered film can be lowered by the diffusion and reaction processes: i.e., the ratio of Sb–Te and Ge–Te bonding is controlled by the diffused Ge. Before the annealing treatment,

the stoichiometry of Sb₂Te₃ was calculated using the peak area of Sb–Te in Sb 4d and Te–Sb in Te 4d and atomic subshell photoionization cross sections.²² After the annealing treatment, the stoichiometry of Ge_{1.2}Sb₂Te₄ was calculated using the Ge–Te peak in Ge 3d and Sb–Te in Sb 4d and the Te–Ge and Te–Sb summed in Te 4d. The value is in excellent agreement with the most stable stoichiometry calculated by ab initio density-functional theory.¹¹ Moreover, the formation of GeTe₂ caused by SP³ bonds, which appeared in an annealed Te(10 Å)/Ge film at 200 °C, is not observed in Te/Sb/Ge. In the case where GeTe₂ contains Sb, the chemical bonding characteristics are changed, resulting in valence electrons favoring P–P bonds, which prevent the occupation of electron in the antibonding state.⁷ The bonding characteristics were observed in our valence band spectrum, as shown in Figure 5c. The valence band spectrum of an as-grown Te(10 Å)/Sb(10 Å)/Ge film has relatively large peaks at 1.49 eV and shoulders at around 2.82 eV and 4.5 eV with respect to the VBM, similar to that of an Sb(10 Å)/Te film annealed at 200 °C. However, in the case of the annealed film, the 4P and 5P orbital structure of Ge, Sb and Te show peaks at 0.73 eV, 2.33 eV and 3.03 eV, respectively, with respect to the VBM in the binding energy region of 0–6 eV. Therefore, the valence band of the near surface in the annealed sample is very similar to the reported valence band spectrum of Ge₁Te₂Te₄ in a metastable crystalline state.¹⁵ Finally, we can conclude that the Ge diffused to the near surface and controlled the vacancy in the metastable crystalline phase, thus leading to a stable state.

Conclusion

In summary, the electronic structure of a Te(10 Å)/Ge film annealed at 200 °C showed that Ge atoms have SP³ hybridization bonds, providing support for the existence of a randomly bonded 4(Ge):2(Te)-coordinated network model of an amorphous GeTe film. Comparing the bonding characteristics of Te(10 Å)/Sb(10 Å)/Ge multilayer with various multilayers composed of layers of Ge, Sb, and Te, the diffused Ge expels Sb in Sb–Te bonds and interacts with residual Te. Finally, the film changes from an unstable state to a more stable state with a specific stoichiometry, which is in good agreement with calculation by ab initio density-functional theory.

Acknowledgment. This research was supported by the National Research Project for the Phase-change Random Access Memory Development and the IT R&D program of MKE/IITA (2008-F-023-01, next generation future device fabricated by using nano-junction) sponsored by the Korean Ministry of Commerce, Industry, and Energy.

Supporting Information Available: X-ray diffraction patterns of [Te(9 Å)/Ge(8 Å)/Te(9 Å)/Sb(8 Å)]₁₅ multilayer film, XPS spectrum of Sb(1, 3, 5, 7 and 10 Å)/Te(150 Å)/Ge film and Te(1, 3, 5, 7 and 10 Å)/Ge film, XPS spectrum of Te(10 Å)/Ge and Te(10 Å)/Sb film annealed at 100, 120, 150, 200 °C and returned to room-temperature. This material is available free of charge via the Internet at <http://pubs.acs.org>.

JA901596H

(19) Sarrach, D. J.; De Neufville, J. P.; Haworth, W. L. *J. Non-Cryst. Solids* **1976**, *22*, 245–267.

(20) Yamada, N.; Matsunaga, T. *J. Appl. Phys.* **2000**, *88*, 7020–7028.

(21) Kim, J. J.; Kobayashi, K.; Ikenaga, E.; Kobata, M.; Ueda, S.; Matsunaga, T.; Kifune, K.; Kojima, R.; Yamada, N. *Phys. Rev. B* **2007**, *76*, 115124.

(22) Yeh, J. J.; Lindau, I. *Atomic Data Nuclear Data Table* **1985**, *32*, 1–155.